Novel rapid high-throughput method of NETosis Induction and Inhibition with physiological triggers and inhibitors

Kieran Zukas[1], Justin Cayford[1], Finley Serneo[1], Andrew Retter[2], Mark Eccleston[1], Theresa K Kelly[1]

1. Volition America, 6086 Corte Del Cedro Carlsbad, CA 92011
2. Guys and St. Thomas NHS Foundation Trust, Lambeth, London, United Kingdom, SE1 7EH

Abstract

Neutrophils, the most abundant white blood cells in humans, play pivotal roles in innate immunity, rapidly migrating to sites of infection and inflammation to phagocytose, neutralize, and eliminate invading pathogens. Neutrophil Extracellular trap (NET) formation in response to pathogens is increasingly recognized as an essential rapid innate immune response, but when dysregulated contributes to pathogenesis of sepsis and autoimmune disease. Current models of NETosis are limited, routinely employing non-physiological triggers that can bypass natural NET regulatory pathways. Models utilizing isolated neutrophils and immortalized cell lines, limiting the complex biology underlying neutrophil activation and NETosis, that occurs in a whole-blood environment. Here we describe a novel, high-throughput ex-vivo whole blood induced NETosis model using combinatorial pooling of native NETosis inducing factors in a more biologically relevant Synthetic-Sepsis™ model. We found different combinations of factors evoked distinct neutrophil responses in the rate of NET generation and/or magnitude of NETosis. Despite inter-donor variability, similar sets of pro-inflammatory molecules induced consistent responses across donors. We found at least three biological triggers, were necessary to induce NETosis in our system requiring either TNF-α or LT-α. To our knowledge, we report the first human *ex-vivo* model utilizing naturally occurring molecules to induce NETosis in whole blood. This approach could be used for drug screening and, importantly, inadvertent activators of NETosis. These findings emphasize the importance of investigating neutrophil physiology in a biologically relevant context to enable a better understanding of disease pathology, risk factors, and therapeutic targets, potentially, providing novel strategies for disease intervention and treatment.

Introduction

Sepsis results from a dysregulated host response to infection and affects over 1.7 million adults annually in the US [1, 2]. Rapid recognition and intervention is critical to avoid progression to septic shock and death. Despite advances in critical care, sepsis remains a major global health burden. New strategies are urgently needed to unravel the intricacies of sepsis pathophysiology, in order to understand individual patient susceptibility and develop more effective diagnostic tools and treatments.

Multiple sepsis etiologies, rapid evolution and systemic impact, have limited progress on novel treatments. Neutrophils represent 50-70% of white blood cells in humans and play a pivotal role in the initial response to infection. Whilst Neutrophils can phagocytose pathogens, they also release extracellular traps to rapidly immobilize pathogens and prevent dissemination. NETosis, first described by Brinkmann et al in 2004 [3], involves the formation of Neutrophil Extracellular Trap (NETs) through rapid decondensation of nuclear chromatin, driven by changes to histone post translational modifications, followed by externalization of web like NETs containing long strands of chromatin and include associated antimicrobial granular enzymes (neutrophil elastase (NE) and myeloperoxidase (MPO)) (**Figure 1A**) [3]. While NETs serve as a vital defense mechanism, mounting evidence suggests that dysregulation and excessive formation can contribute to pathogenesis in sepsis and other inflammatory disorders through host directed bystander effects, initiation of a hyperinflammatory feedback loop and Disseminated Intravascular Coagulation [4]. Elevated nucleosome levels, a component of NETs, have been described in several studies of NETosis related conditions including COVID-19 and sepsis, and are negatively correlated with survival [5-8].

NETosis research has largely relied on mouse models, *in-vitro* models using isolated primary neutrophils or neutrophil-like cells induced from immortalized cell lines [9-11]. While these models have provided valuable insights into NETosis, they have significant limitations. Murine immune responses, though informative, can differ substantially from human responses in part due to the significantly lower proportion of neutrophils, their maturation profile and half-life [12-14]. Immortalized HL-60 cells are highly dependent on culture conditions and do not recapitulate neutrophil fragility. NETosis induction in isolated primary neutrophils overcomes many of these limitations providing important insights into neutrophil activation and regulation [15-17]. However, neutrophils are very fragile and the method of isolation impacts their response to various stimuli [18]. To bridge the gap between existing models and the clinical reality of human sepsis, relevant *ex vivo* human models that enable rapid processing and require minimal handling are essential [14].

Various synthetic, as well as physiologically relevant factors induce NETosis. *In-vivo*, Staphylococcus aureus and Lipopolysaccharides (LPS) are commonly used NETosis inducers, while *in-vitro* models typically use LPS or Calcium Ionophore (CI) and, the most commonly reported inducer, phorbol 12-myristate 13-acetate (PMA) [19]. PMA is an extremely powerful inducer of NETosis but is not physiologically relevant as it can bypass natural regulatory pathways governing NET production, thus preventing the ability to understand full regulatory feedback loops, limiting the clinical relevance of findings from PMA induced studies [20].

An *ex-vivo* human NETosis model using physiologically relevant triggers in the presence of other blood cells (e.g. macrophages, platelets) and circulating proteins offers several distinct advantages. Primarily, investigation of the dynamics of NET formation, regulation and function in a clinical context would better translate insights to patient settings. Additionally, human cell models enable exploration of patient-specific factors including genetic predisposition and influence of pre-existing conditions, which can significantly impact sepsis outcomes. By

dissecting the molecular mechanisms underlying NETosis using human cells, we can potentially identify novel therapeutic targets and develop personalized sepsis treatment strategies.

Here, we developed a human primary cell-based Synthetic-Sepsis™ model using intact whole blood to study NETosis induction with physiologically relevant molecules. We show NETosis induction using panels of pro-inflammatory molecules varied in both time-scale and magnitude of NET release compared to non-physiological PMA induction. Furthermore, we show differential NETosis profiles based on specific combinations of molecules, which we hypothesize could distinguish between beneficial and pathogenic NETosis. Moreover, we show that TNF-α or LT-α was necessary but not sufficient for NETosis induction and that in the presence of C5a, rapid onset of NETosis occurred within two hours of exposure. A minimal combination of LT- α, C5a and fMLP was able to consistently induce NETosis in multiple donors. We believe our novel model could delineate underlying complexities of NETosis, potentially leading to the development of innovative diagnostic tools and targeted interventions for sepsis and other NETosis related pathologies.

Results

NETosis Induction and real-time monitoring in whole blood and isolated neutrophils

We set out to develop a more biologically relevant NETosis model than isolated neutrophils. Our approach allows the investigation of NETosis neutrophils in whole blood either in a low throughput, Synthetic Sepsis™, or high-throughput screening approach (**Figure 1A**). We first validated our NET quantification approach, using extracellular DNA intercalation and fluorescence, in a classical isolated neutrophil model of NETosis. A dose dependent increase in DNA release measured by Cytotox green was seen in response to PMA in an Incucyte S3 incubated imaging platform (Sartorius), with signal onset after 2 hours of treatment (**Figure 1B**). Treatment with the MPO inhibitor, ABAH, substantially delayed the onset of DNA release and reduced the overall level of release, consistent with NETosis inhibition (**Figure 1C**). The results were confirmed by fluorescent microscopy at 6 hours post PMA treatment (**Figure 1D**). CI and LPS, established NETosis inducers, also induced NETosis in isolated neutrophils in a dose dependent manner (**Figure 1E and Figure 1F**).

To study NETs in a more biologically relevant system, (i.e. in the presence of other blood proteins and cell types) we incubated whole blood in EDTA tubes from two healthy donors with PMA, CI or LPS. NETosis was quantified by nucleosome release and H3.1 nucleosome levels started to increase three hours after treatment with PMA (**Figure 1H**). Differential nucleosome elevation was seen in both donors over the time course. Only PMA induced NETosis in whole blood, unlike in isolated neutrophils, where all three molecules induced NETosis (**Figure 1G**). This unexpected finding suggests that isolated neutrophils respond differently than whole blood.

High-throughput model for NETosis induction

To identify physiologically relevant NETosis activators we adapted the model for high-throughput screening. As neutrophils are fragile, we designed a rapid screening format with limited handling utilizing a MANTIS liquid dispenser (Formulatrix) to distribute molecules across a 384-well plate followed by 50 µl aliquots of EDTA whole blood containing sytox green per well (**Figure 2A**). The plate was centrifuged to sediment erythrocytes leaving an upper plasma layer and buffy coat containing neutrophils at the interface (**Figure 2A**). NET formation was measured from the top through the plasma via intercalation and fluorescence of extracellular DNA using a SpectraMax plate reader.

To evaluate consistency across the plate and limit potential artifacts (edge effects, temperature variation and oxygenation), a series of optimizations were performed across an entire 384 plate using 250 nM of PMA to induce NETosis (**Figure 2B**). Experimental parameters were optimized to ensure that small changes in fluorescent intensity at the onset of NETosis could be reliably detected. The time of NETosis (t_{NET}), was calculated as the time at which the fluorescent signal exceeded 3.3 × the standard deviation of a vehicle treated control group. Assay optimization focused on reducing the standard deviation in t_{NET} to +/- 5 minutes across the plate. We performed a randomized PMA titration across the entire plate and showed a dose response curve of NETosis induction (**Figure 2C**). Nucleosome release was measured in plasma isolated from treated whole blood in parallel using the H3.1 Nu.Q® NETs assay (Volition) and showed the time course of nucleosome release was consistent with the Sytox green signal (**Figure 2D**). In this high-throughput, induced NETosis model we found that both CI and LPS failed to induce NETosis (**Figure 2E and Figure 2F**), reflecting the results seen in whole blood (**Figure 1G**). MPO inhibition (ABAH) delayed the onset of NETosis (**Figure 2F**) consistent with the inhibition of NETosis, as noted in isolated neutrophils.

Variability of NETosis Profiles

The high-throughput NETosis model was used to screen candidate NETosis regulators selected based on reported association with NETosis or neutrophil biology (Table 1). Design of Experiments (DOE) was performed to combine selected factors in an iterative screen to identify the minimal candidate pool required to induce DNA release (**Figure 3A**). Initially, 6-19 factors were combined into individual wells with each factor represented in approximately half of the wells. Four distinct fluorescence patterns were observed following treatment with the various combinations: no response; initial response with early plateau; delayed response with continued gradual increase and initial response with secondary response with continued increase (**Figure 3B**). To assess the relative contribution of each factor to the fluorescence signal at each time point, we averaged the raw signal over 30-minute windows, calculated the first derivative, and performed multivariate regression modeling (**Figure 3C**). The contribution of each factor across each of the wells was used to determine the potential extent the specific factor contributed to the signal. Figure 3d shows examples of four observed patterns: C5a and TNF-α contributed to a rapid onset of DNA release, with TNF- α having a secondary protracted effect on the system. Interleukin-5 (IL-5) did not appear to have a significant impact on fluorescence signal and Interleukin-1β (IL-1β) appeared to reduce the fluorescence signal, indicating potential inhibition or buffering capacity. We performed two rounds of screening in

blood from two different healthy donors (n=4) and found that TNF-α, LT-α, IFN-γ, GM-CSF, LTB4, C5a, and Ferritin consistently contributed to increased Sytox Green signal across donors whereas LPS and fMLP only contributed in one of the two screens (**Figure 3E**). Molecules with negative or no effect on signal were removed for subsequent NETosis inducer screens. Ferritin was observed to consistently contribute to an increase in signal but was removed from subsequent screens as it was horse derived.

Biological Relevant NETosis Induction Consistency Across Donors

Levels of endogenous cytokines vary across individuals and in response to environmental stimuli contributing to natural variability in innate immune response. Inter and intra donor variability of NETosis induction was evaluated using the eight selected factors. To normalize the effect each combination of factors had across donors: we performed a Boolean transformation of the first derivative change in RFU over the time course with a cutoff at 3.3 SD × of the background signal (**Figure 4A**). We tested combinations of the selected 8 factors (TNF-α, LT-α, IFN-g, GM-CSF LTB4, C5a, LPS, and fMLP) in six donors and found signal consistently increased across donors with more factors (**Figure 4B**). Four factors increased NETosis in most of the six donors tested with two distinct patterns: early onset between 30 minutes and two hours, followed by a later increase after three hours. Female donors were generally less responsive than males, especially with earlier onset NETosis (**Figure 4C**). Either TNF-α or LT-α was required for consistent increase in signal across donors. In their absence, the remaining six compounds failed to induce consistent signal (**Figure 4D**). Interestingly, C5a or LPS appeared to be critical for the early onset signal (30 minutes to 2 hours) (**Figure 4D**). To investigate the relative role of each factor, we selected a pool of five factors (LT- α, GM-CSF, C5a, LPS, and fMLP) which induced early DNA release in all donors tested but not the later release, hypothesizing that the secondary response could reflect mechanisms other than NETosis. The impact of each factor in combination with the other factors across the six donors is shown in **Figure 4E**. These results highlighted differences between male and female donors, for example, it appeared GM-CSF and LPS were less important for the early response in males compared to females and that male donors were more likely to undergo NETosis with less stimulation compared to the female donors with the five factor pool.

Minimal factors required for NETosis induction

To determine whether individual donors responded to the same combination of compounds over time we had two donors undergo multiple blood draws over a month period and found general consistency for NETosis initiation with the five factor pool (LT- α, GM-CSF, C5a, LPS, and fMLP) across and within donors, with a pool of LT-α, C5a and fMLP giving the most consistent result with the fewest number of factors (**Figure 5A**). Variability was reduced as more factors were utilized, however we observed a possible set of three factors (LT- α, C5a, and fMLP) which had consistency and similar results as those pools which included either GM-CSF and or LPS. Due to this, space-filling DOE and Gaussian Process Regression was used to evaluate the concentration dependence of each factor in blood samples from two healthy donors. We found that GM-CSF did not play a significant role in either donor, while LPS appeared to decrease the

overall observed signal in a dose-dependent manner (**Figure 5B**). Consequently, we removed GM-CSF and LPS from the pool to generate the minimal combination of factors required to induce an increase in NETosis.

All three remaining factors were required to generate an increase in Sytox Green signal (**Figure 5C**), with the EC50 of each being consistent with published values for neutrophil activation **(Table 2)**. To confirm the signal we were seeing upon treatment with these natural triggers was a result of NETosis, we treated whole blood with the optimized concentrations of LT-α, C5a, and fMLP, along with a variety of inhibitors. We showed a significant decrease in signal when inhibitors targeting Neutrophil Elastase II, protein arginine deiminase (PAD), and PAD4 were included (**Figure 5D**). However, there was no change in signal when an apoptosis inhibitor (Caspase 3/7 inhibitor I) or necroptosis inhibitor (necrostatin-1) were included. This evidence suggests the increased signal from sytox green was a result of NETosis and not an alternative form of cell death. We did see a marginal, yet not significant decrease in DNA release upon treatment the MPO inhibitor (ABAH), suggesting that NETosis induction using these natural triggers may be different than what is seen with PMA.

Discussion

Sepsis is a major global disease. There are an estimated 48.9 million cases annually and 11 million sepsis related deaths [21]. Additionally, patients who recover from sepsis are at greater risk of readmission to hospital and have a greater risk of death when compared to age and sex-match controls [22]. A key driver for pathogenesis and potentiator of sepsis is excessive NET formation [23]. Physiologically relevant models mimicking endogenous NETosis enable mechanistic investigation of the complex signaling cascades underlying NETosis activation. Our representative *ex-vivo* model of these cascades offers the opportunity for screening therapeutic interventions under disease mimetic conditions which reflect underlying conditions which may predispose patients to adverse outcomes. To our knowledge, we show for the first time the *ex-vivo* induction and real time kinetic read out of NETosis using naturally occurring molecules in a whole blood system. We found that activation with TNF-α or LT-α was required for rapid onset NETosis, highlighting the importance of these molecules in sepsis. Indeed, TNF-α has been shown to be elevated in sepsis and is a putative therapeutic target [24].

Interestingly, we found that CI, and LPS showed a differential ability to induce NETosis in whole blood compared to isolated neutrophils, which could be due to the presence of an additional cell type or factor present in whole blood, and reflects the complexity of the whole blood model compared to isolated neutrophils. Mol et al, previously reported that treating neutrophils with pairs of factors similar to what we identified (GM-CSF, fMLF, TNF, and LPS), resulting in neutrophils displaying a variety of neutrophil associated behaviors (e.g. ROS production, degranulation, phagocytosis) but they were not able to induce NETosis [17]. Our ability to induce NETosis in our *ex-vivo* model using no less than three different factors, demonstrates the complex signaling needed for NETosis to occur, and suggests that there is something present in whole blood that support NETosis. Whole blood has a variety of proteins

and other cells types (e.g. platelets and macrophages) which are known to induce NETosis and additional work is necessary to determine whether these cells play a role in the NETosis we observe in our *ex vivo* model.

NETs play a critical role as part of the innate immune response to infection, immobilizing pathogens to prevent dissemination and clearing them from circulation [23]. However, excessive NETosis can be pathogenic and lead to host directed bystander effects and thrombosis [25]. Thus, NETosis can be both beneficial and detrimental [25]. The differential time courses and magnitudes of NETosis seen in our *ex-vivo* whole blood model in response to specific combinations of pro-inflammatory compounds may be correlated to beneficial vs pathogenic NETosis (**Figure 3B**). It is possible that the compound combinations in which the amount of NETosis was minimal represents the beneficial NETosis, whereas conditions that led to higher release may reflect pathogenic NETosis. Furthermore, some combinations trigger a biphasic release pattern with a moderate early minimal response followed by a secondary exacerbated response, which could be reflective of a positive feedback loop in which nucleosomes released from the early NETs further stimulate additional NETosis [26]. These patterns provide an opportunity for biomarker identification as well as therapeutic intervention for future study.

In our initial screens we found that pools with molecules that interact with similar cell-surface markers/signaling cascades induced consistent responses across donors, which suggested a potential convergence of required signaling pathways. At least three naturally occurring factors in combination (LT-α, fMLP and C5a) were necessary to consistently induce NETosis in our system indicating a potential requirement of the activation of TNF Receptor 1, TNF Receptor 2, or LT-β receptors for NETosis to occur [27]. NETosis induction did not occur in the absence of TNF-α or LT-α, underlying the potentially significant roles these factors play in inflammatory disease, and suggests an underlying master regulatory mechanism, such that certain factors are essential but not individually sufficient to trigger NETosis.

These findings emphasize the importance of expanding the understanding of neutrophil physiology in a biologically relevant context. Physiological triggers of NETosis could be used to better understand NET associated disease pathology, risk factors, and potential therapeutic targets, providing novel strategies for disease intervention and treatment. Our novel *ex-vivo* NETosis approach has the potential to be used for screening drug candidates as inhibitors and inadvertent activators of NETosis and through a comprehensive exploration of human cell-based NETosis, we can take significant strides toward mitigating the devastating impact of sepsis on global healthcare.

Methods

Neutrophil isolation & Imaging

Anonymous healthy donor K2-EDTA whole blood was obtained from PrecisionMed (San Diego, USA; WCG IRB Protocol number 20181025), stored at room temperature, and processed within

one-hour post-draw. Neutrophils were isolated using the MACSxpress Whole Blood Neutrophil Isolation Kit (Miltenyi, 130-104-434) and resuspended in RPMI (Gibco, 11-875-119) containing 250nM Cytotox Green (Sartorious, 4633) to 2.0 x 10^5 cells/mL and seeded at 100µL/well in a 96-well Incucyte ImageLock plates (Sartrious, 4806) coated with 10µg/mL Fibronectin (Sigma-Aldrich, F1141). The plate was centrifuged at 120*g* for two minutes to seat the neutrophils at the bottom of the plate. NETosis stimuli and inhibitors were diluted in RPMI containing Cytotox Green then added to the neutrophils to the indicated final concentration. Inhibitors were incubated with neutrophils at 37°C for one hour before adding stimuli. NETosis was analyzed using Incucyte's S3 Live-Cell Analysis System (Sartorious). The plate was imaged every 20 minutes using phase contrast and green fluorescent exposure channels and a 10× objective. Neutrophils were identified by phase contrast, objects smaller than 30 μm^2 were excluded. Positive NETosis (Green) signal was optimized for measuring total area with Top-Hat for background correction and Edge Split Off.

NETosis Induction in Whole Blood

Anonymous healthy donor K2-EDTA whole blood was obtained from PrecisionMed (San Diego, USA), with samples stored at room temperature and processed within one-hour post-draw. Blood was treated with 0.625µL/mL of $CaCl_2$ solution (5mM in ddH_2O) and mixed. Pooled blood was treated with either PMA (Sigma Aldrich, P1585), or vehicle (DMSO) followed by inversion mixing. Each condition was aliquoted into 2mL low protein binding tubes (Cat#90410, Thermo Scientific) and incubated at 37°C under rotation at 10 RPM. Plasma was isolated from treated blood at designated time points by centrifugation in a swinging bucket rotor for 10 minutes at 1300 x g with no brake at room temperature. Plasma fractions were transferred and nucleosomes measured in duplicate using the H3.1 Nu.Q® NETs immunoassay (Belgian Volition).

Screening

Whole blood screening candidates were selected based on literature reports of an association with NETosis (Supplementary Table 1). Concentrations were equivalent to or in excess of commonly used for *in-vitro* stimulation. Recombinant lyophilized proteins were resuspended using 0.1% (w/v) human serum albumin (HSA) (A9731, Sigma-Aldrich) in sterile water, with further dilutions of reagents made using 0.1% HSA in PBS. Reagents were dispensed in plates (3575, Corning) using the Mantis V3 Liquid Handler (Formulatrix) with Silicon LV or PFE LV chips (233581 or 233129, Formulatrix). Wells were backfilled with appropriate solvents (Ethanol, DMSO, 0.1% HSA in PBS), such that the concentration and volume of vehicle was consistent across wells. Plates contained 6 wells of each the following controls: untreated, PMA (50, 250, and 500 nM) randomly distributed across the plate to assess assay performance. The factors contained within remaining wells were determined by the optimal DOE screening design computed using JMP V17.1 (JMP Statistical Discovery).

Fluorescent Plate Assay

50 µL of oxygenated whole blood was dispensed across a prepared 384-well fluorescent assay microplate using the Mantis Continuous Flow Silicon Chip (233127, Formulatrix). After

dispensing, the plate was sealed (235307, Thermo Scientific) and mixed (orbital shaking) at 1400RPM for 10 seconds. Plates were then centrifuged at 1300 x g for 10 minutes at room temperature using a swinging bucket rotor, without braking. Centrifuged plates were pre-heated to 37°C on a dry-heat block (25-038A, Lonza) for 15 minutes prior to reading.

Kinetic fluorescent measurements were obtained using a SpectraMax iD5 Multi-Mode MicroPlate Reader (Excitation = 510nm, Emission = 550nm), top read, at two minute sampling intervals for 24 hours. For inhibition studies, inhibitors, vehicle, and backfill were added to the wells followed by oxygenated whole blood and incubated at room temperature for 45-60 minutes after which PMA or physiological molecules were dispensed, the plate was sealed, and the assay continued as described above.

Screening Design and Statistical Analysis

Optimal screening design was computed using JMP V17.1 (JMP Statistical Discovery) custom screening design, with all main effects and fourth degree interactions included, but assigned estimatibility to "if possible". The number of runs specified for each plate was set to 360 with no additional center points or replicate runs. RFU signal was averaged into 30-minute intervals, followed by calculating the change in the smoothened RFU values at 30-minute intervals. These values were used for input into multivariate regression modeling using JMP V17.1, with the concentration of each molecule in each treatment being the dependent variable, and each change in RFU value at 30 minute intervals being the independent variable. The effect of each factor was assessed by t-test to determine if the predicted coefficient at any given period was non-zero, and if the factor was acting to increase or decrease signal at any given time. Factors with a significant non-zero effect on the signal and acted to increase signal over time ($P < 0.1$) in one or both tested donors for that screen, were selected to move forward for additional screening.

Dose-Response profiles for the three-factor combination were characterized by space-filling DOE (JMP V17.1). The selected design was sphere-packing optimal with 88 different concentration combinations of LT-α, C5a, and fMLP and tested in triplicate. The system's dose-response surface was generated using gaussian process regression and gaussian correlation structure, with nugget parameter estimation. Each individual factor's EC50 was obtained by determining the log concentration at the signal half-max for each factor, given that the two other factors are at their maximal concentrations.

Table 1

Comparison of Literature EC50 Values and Experimentally Determined ED50 Values			
Factor	**Source**	**Literature EC50 Values**	**Experimental EC50 Values**
LT-α	Reported various cell types (not neutrophils)	-2-0 ng/mL	-0.6 (+/-0.8) ng/mL
C5a	Isolated neutrophils Chemotaxis [28]	1.88 ng/mL	2.2 (+/-0.4) ng/mL
fMLP	Isolated neutrophils ROS production [29]	1.34 ng/mL	1.8 (+/-0.5) ng/mL

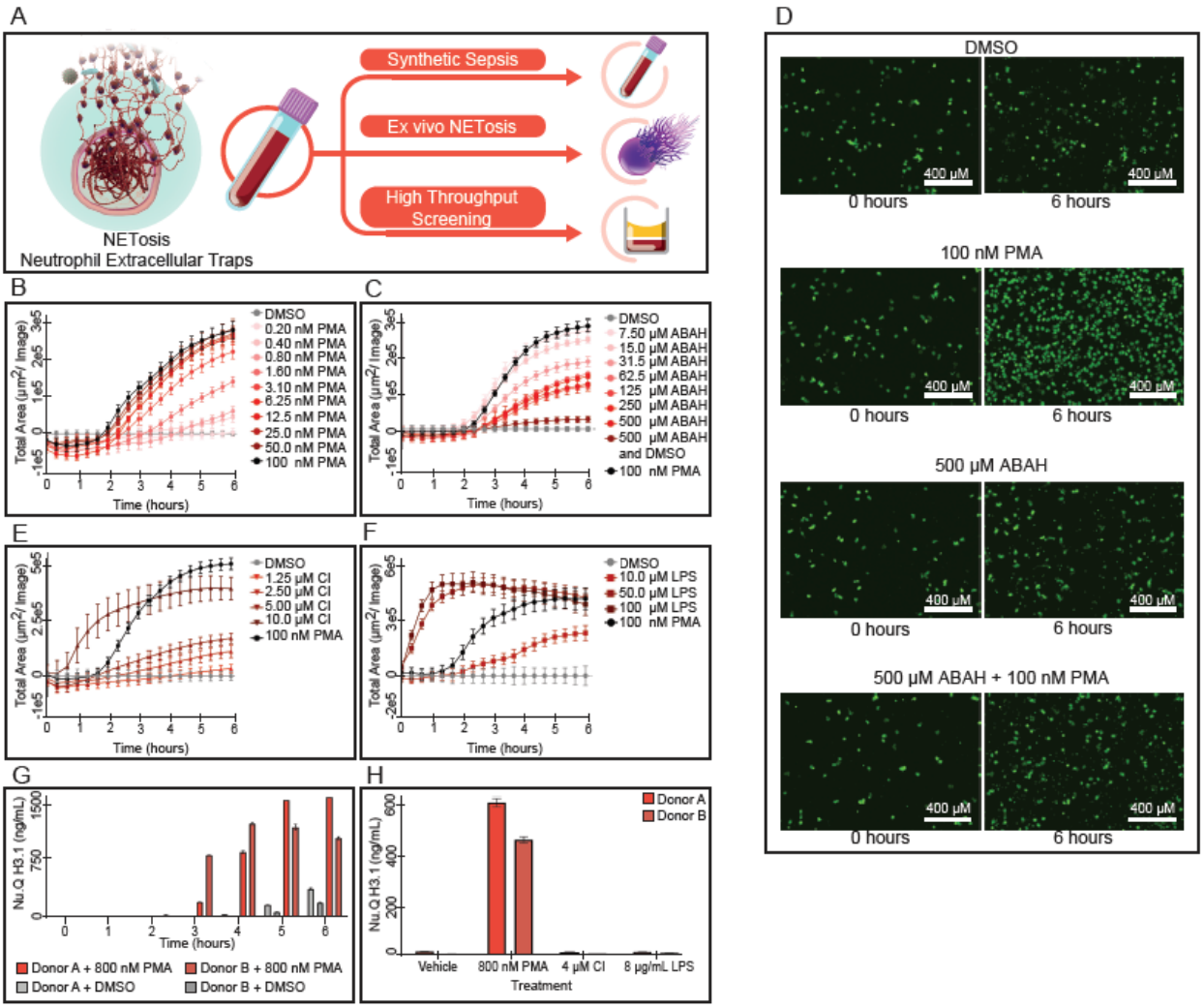

Figure 1 | Induction of NETosis in a whole-blood system with H3.1 Nu.Q® and Incucyte Systems: (A) Diagram of how we measure NETosis using our Synthetic Sepsis™, *ex-vivo*, or high-throughput screening methods. (B) PMA titration (•) and a DMSO control (grey •) on primary isolated neutrophils using Cytotox green dye (Sartorius #4633) on an S3 Incucyte imaging system from Sartorius. (C) Similar to Fig 1B, but isolated neutrophils were first incubated with MPO inhibitor (ABAH) (various colors •), a DMSO control (grey •), and 100 nM PMA (black •). (D) Representative images from the Incucyte system for Fig 1C. These were taken at the start of the assay (left panels) and after six hours (right panels). The scale bars indicate 400 µm. (E) Similar to Fig 1B, but isolated neutrophils were treated with various concentrations of CI (▾) and compared to a DMSO control (grey •) and 100 nM PMA (black •). (F) Similar to Fig 1B and Fig 1E, but isolated neutrophils were treated with various concentrations of LPS (■) and compared to a DMSO control (grey •) and 100 nM PMA (black •). (G) Whole blood was treated with either 800 nM PMA (red ■) or DMSO (grey ■) and measured for H3.1 Nu.Q® over six hours indicating the ability to capture NETosis. (H) Whole blood from two donors was treated with the indicated

concentrations of a vehicle control, PMA, CI, or LPS for four hours and measured with H3.1 Nu.Q®.

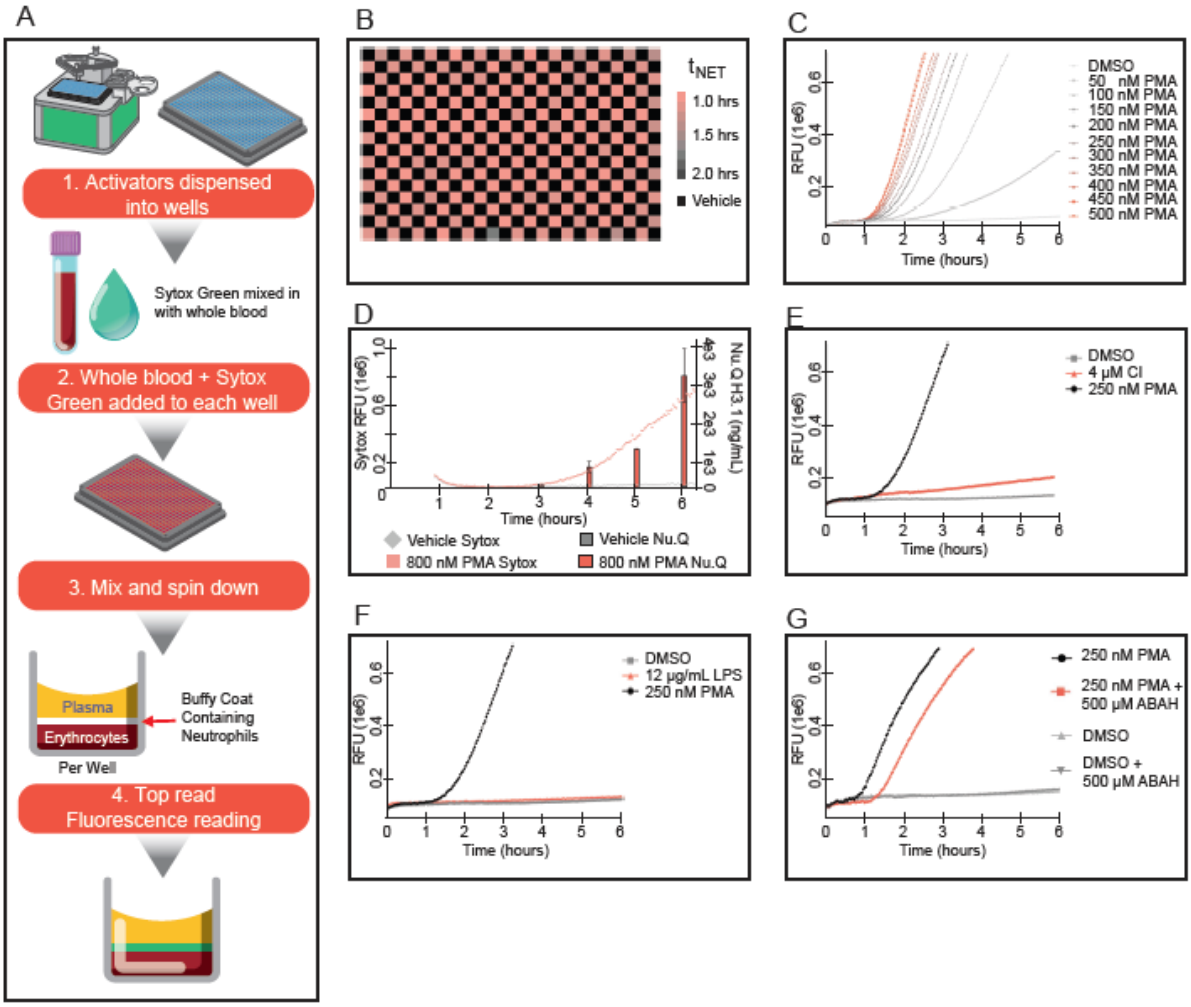

Figure 2 | High-throughput *ex-vivo* method of screening NETosis in whole-blood: (A) Workflow for the *ex-vivo* system. Briefly, reagents excluding whole-blood are dispensed into a 384-well plate using the MANTIS system (Formulatrix). Whole blood is mixed with Sytox Green (ThermoFisher #S7020) and then dispensed into the same plate. The plate is mixed and spun down to separate plasma and erythrocytes. Finally, top read fluorescence is completed. (B) The assay used 250 nM PMA to activate NETosis and the time of NETosis (t_{NET}) was measured to show consistency across the assay plate. (C) PMA titration (various colors: ▲, ▼, ■, ●, ♦) and a DMSO control (grey ●) was completed over six hours. (D) The high-throughput method was compared to H3.1 Nu.Q®, where Sytox signal can be seen on the left axis and Nu.Q signal on the right axis. A vehicle control (grey ♦) and 800 nM PMA (light red ■) indicate sytox green RFU from the high-throughput model. A corresponding vehicle control (grey ■) and 800 nM PMA (red ■) indicate measurements from H3.1 Nu.Q® readings (ng/mL). (E) Similar to Fig 2C, but 250 nM PMA (black ●) was compared to treatment with 4 µM CI (▲), and a DMSO control (grey ●). (F) Similar to Fig 2E, but 250nM PMA (black ●) was compared to treatment with 12 µg/mL LPS

(▲), and a DMSO control (grey •). (G) Similar to Fig 2E and Fig 2F, but 250 nM PMA (black •) was compared to treatment with 250 nM PMA with 500 µM ABAH (■). Also included was a DMSO control (▲) and a DMSO control with 500 µM ABAH (▼). The whole blood was incubated for 45 minutes with or without the ABAH added prior to addition of PMA.

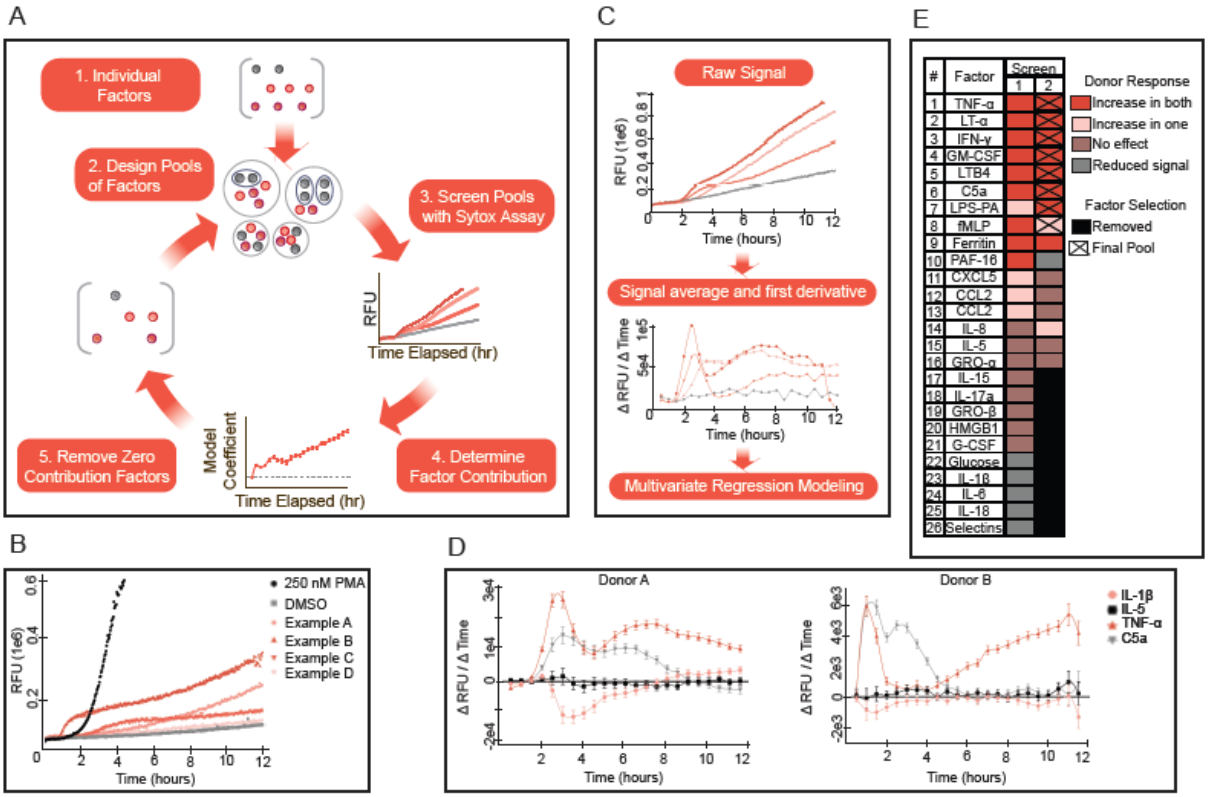

Figure 3 | Selection of naturally occurring chemokines and cytokines using sequential pooling: (A) Design of the multi-factor screening process. Briefly, individual factors were selected and then pooled. The pooled factors were then tested using the high-throughput screening method and Sytox Green (ThermoFisher #S7020) signal was measured. The contribution of each factor was determined and factors which did not increase NETosis were removed, and the new pools were designed. (B) There were four distinct signal profiles for the various pools. The distinct signals were compared to a DMSO control (■) and 250 nM PMA (•). Example A (dark ♦) showed delayed response with continued gradual increase, Example B (▲) initial response with secondary response with continued increase, Example C (▼) showed an initial response with early plateau, and Example D (light ♦) showed no response. (C) Analysis workflow. Raw signal was averaged over 30-minute windows followed by the first derivative. Afterwards, multivariate regression modeling was completed to determine factor contributions in each pool. (D) An example of the multivariate regression (Fig 3C), highlighting four common factors: IL-1β (•) showed less NETosis signal, IL-5 (■) had limited response, C5a (▼) and TNF-α (▲) showed a high amount of contribution to the NETosis signal. (E) The full list of factors tested and their responses. Two unique donors were tested in each screen and the final pool was indicated with an X.

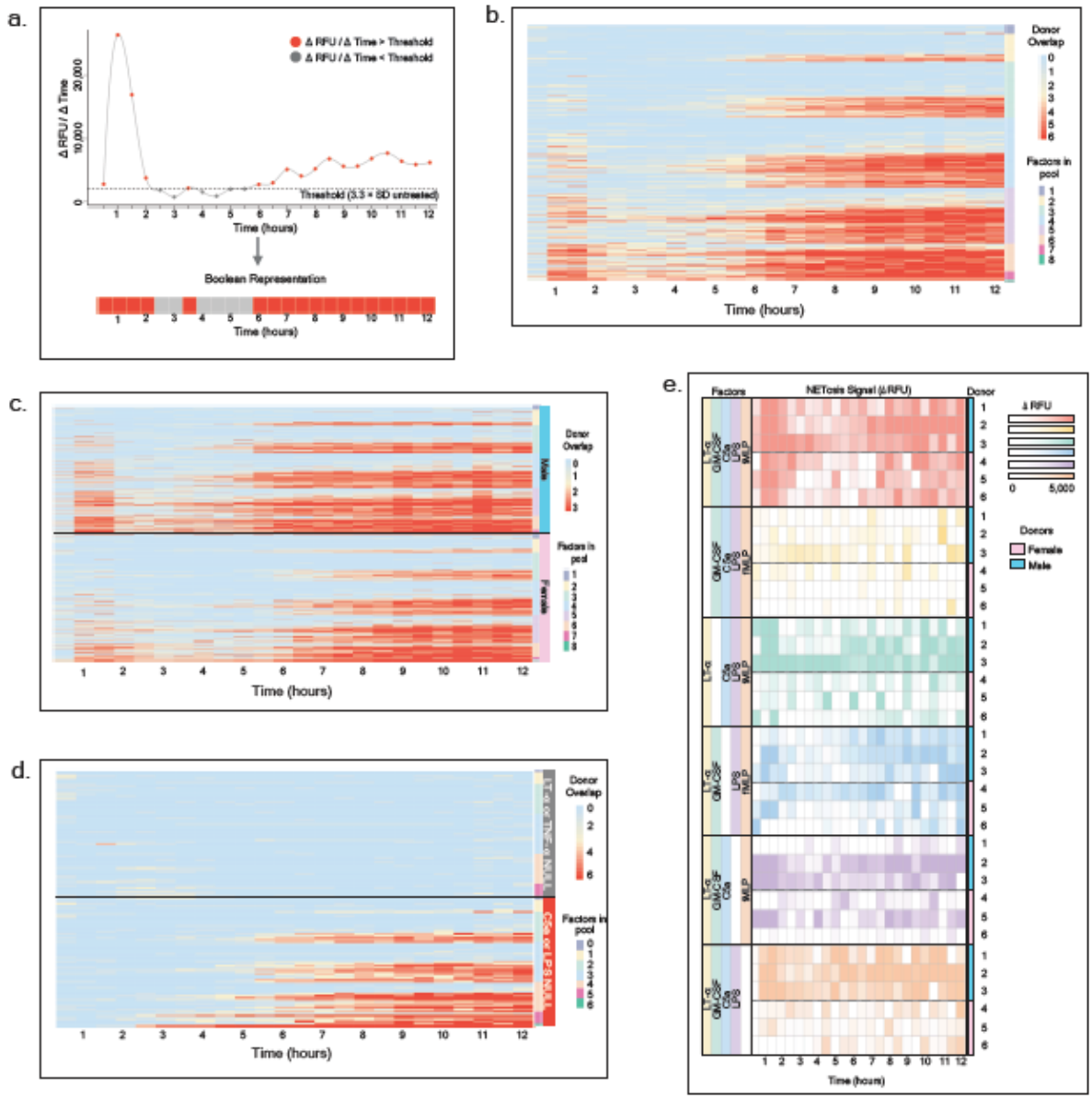

Figure 4 | Understanding of the 8-factor pool and determining minimal factor pool needed for NETosis: (A) Example of Boolean (binary) representation of the first derivative NETosis signal. If signal was above the threshold (3.3 × Standard Deviation of Vehicle Signal – dashed line), it was marked as positive (red •) and converted to a 1, otherwise it was marked as negative (grey •) and converted to a 0. (B) Boolean representation of NETosis signal over six healthy donors. The factors were pooled in a full factorial manner, such that all possible combinations were present and indicated by the number of factors in each pool. (C) Similar to Fig 4B, but donors were broken up between male (blue bar) and female (pink bar). (D) Similar to Fig 4B and Fig 4C but removing either LT-α and/or TNF-α (top – grey bar) or C5a and/or LPS (bottom – red bar). The overlap of the donors showed limited NETosis without LT-α and/or TNF-α. (E) Using a limited pool of 5 factors (left panel), the change in NETosis signal over background signal is shown (right panel). Sequential removal of one factor is shown in each colored panel on the right, where

each row is an individual donor. For each colored panel (right), the donors are kept in the same order. Red indicates all factors present, yellow removed only LT-α, green removed only GM-CSF, blue removed only C5a, purple removed only LPS, and orange removed only fMLP.

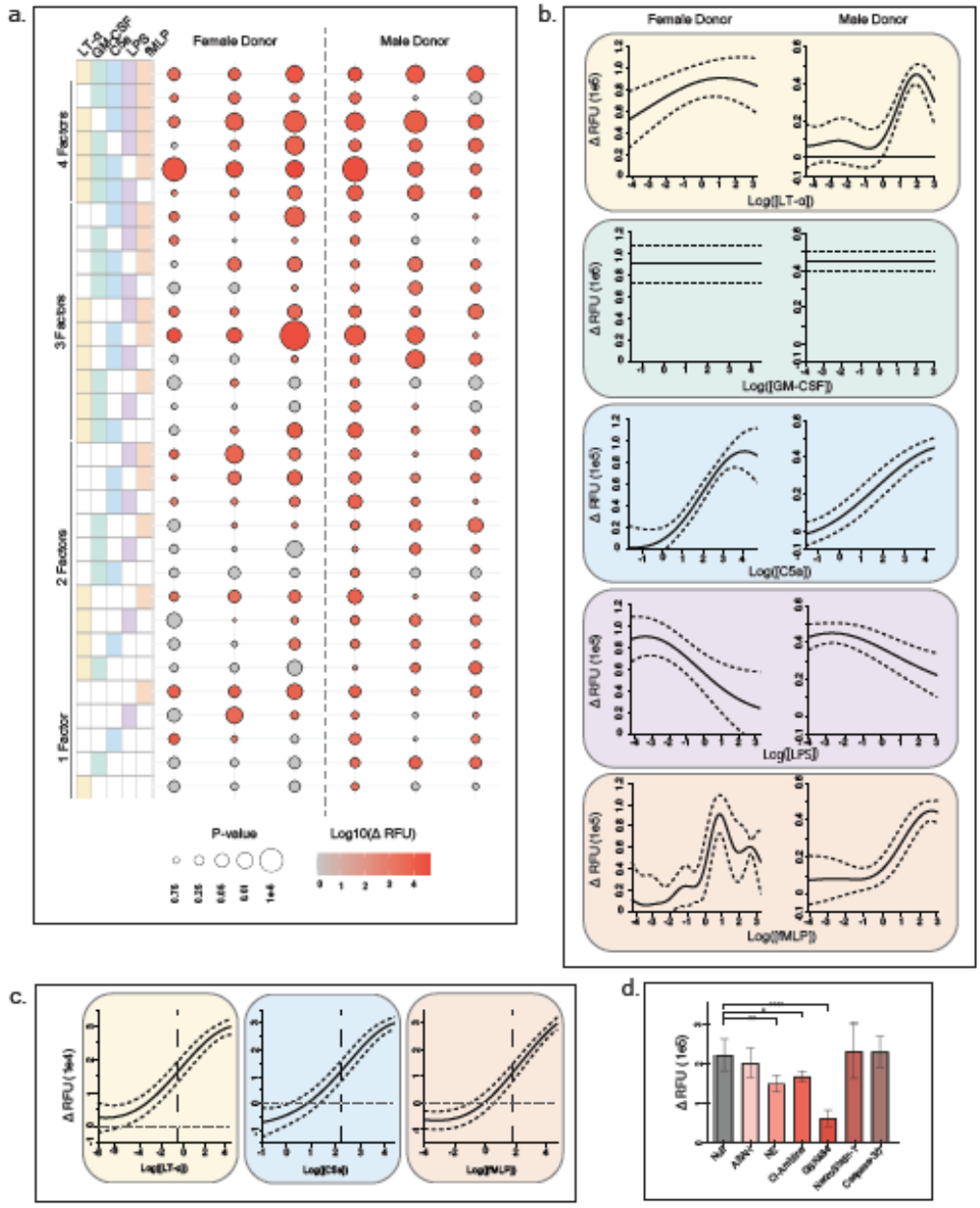

Figure 5 | Determination of minimal factors required to induce NETosis in the *ex-vivo* system: (A) A male and female donor were tested over three time points (over 30 days) with a full factorial of the five-factor pool from Fig 4E (LT-α, GM-CSF, C5a, LPS, and fMLP). Factors are indicated on the left panel where the filled in color denotes the factor was present in that row (LT-α – yellow, GM-CSF – green, C5a – blue, LPS – purple, and fMLP – orange). Decreasing p-value is indicated by increasing circle size and raw change in the NETosis signal (RFU) after 4 hours is shown in the color. (B) Various concentrations of the five-factor were tested on the

same male and female donors were completed to determine optimal concentrations required for induction of NETosis. Delta RFU after 4 hours is shown on the y-axis and log concentration of the factors (ng/mL) is shown on the x-axis. 95% confidence is shown as dashed lines. The factors were colored as before (LT-α – yellow, GM-CSF – green, C5a – blue, LPS – purple, and fMLP – orange). (C) EC50 concentrations were determined after removing the two factors which showed limited response (GM-CSF and LPS). 95% confidence is shown in the dashed line. The calculated EC50 values indicated by a vertical dashed line were: LT-α: -0.6 ± 0.8 ng/mL, C5a: 2.2 ± 0.4 ng/mL, and fMLP: 1.8 ± 0.5 ng/mL. The factors were colored as before (LT-α – yellow, C5a – blue, and fMLP – orange). (D) Using the pool of three factors at the optimized EC50 concentrations, inhibitors targeting the following were compared to a Null treatment: 280 µM MPO (ABAH - Sigma #A41909-10G), 65 µM NE (NEi II - Sigma #324744-5MG), 350 µM pan-PAD (Cl-Amidine - Sigma #506282-10MG), 25 µM PAD4 (GSK484 - Sigma #SML1658-5MG), 40 µM Receptor-interacting protein kinase 1 (NecroStatin-1 - Sigma #), and 15 µM Caspase 3/7 (Sigma # 218826-1MG). * indicates $p > 0.05$, ** indicates $p > 0.005$, and **** indicates $p > 5e-5$.

References

1. https://www.cdc.gov/sepsis/index.html.
2. Singer, M., et al., *The Third International Consensus Definitions for Sepsis and Septic Shock (Sepsis-3).* Jama, 2016. **315**(8): p. 801-10.
3. Brinkmann, V., et al., *Neutrophil extracellular traps kill bacteria.* Science, 2004. **303**(5663): p. 1532-5.
4. Popescu, N.I., C. Lupu, and F. Lupu, *Disseminated intravascular coagulation and its immune mechanisms.* Blood, 2022. **139**(13): p. 1973-1986.
5. Chen, Q., et al., *Circulating nucleosomes as a predictor of sepsis and organ dysfunction in critically ill patients.* Int J Infect Dis, 2012. **16**(7): p. e558-64.
6. Duplessis, C., et al., *Evaluating the discriminating capacity of cell death (apoptotic) biomarkers in sepsis.* J Intensive Care, 2018. **6**: p. 72.
7. Cavalier, E., et al., *Circulating Nucleosomes as Potential Markers to Monitor COVID-19 Disease Progression.* Front Mol Biosci, 2021. **8**: p. 600881.
8. Morimont, L., et al., *NETosis and Nucleosome Biomarkers in Septic Shock and Critical COVID-19 Patients: An Observational Study.* Biomolecules, 2022. **12**(8).
9. Kenny, E.F., et al., *Diverse stimuli engage different neutrophil extracellular trap pathways.* Elife, 2017. **6**.
10. Blanter, M., M. Gouwy, and S. Struyf, *Studying Neutrophil Function in vitro: Cell Models and Environmental Factors.* J Inflamm Res, 2021. **14**: p. 141-162.
11. Nakayama, T. and H. Saitoh, *Tunicamycin-induced neutrophil extracellular trap (NET)-like structures in cultured human myeloid cell lines.* Cell Biol Int, 2015. **39**(3): p. 355-9.
12. Simon, S.I. and M.-H. Kim, *A day (or 5) in a neutrophil's life.* Blood, 2010. **116**(4): p. 511-512.
13. Arpinati, L., et al., *NETosis in cancer: a critical analysis of the impact of cancer on neutrophil extracellular trap (NET) release in lung cancer patients vs. mice.* Cancer Immunol Immunother, 2020. **69**(2): p. 199-213.
14. Nauseef, W.M., *Human neutrophils ≠ murine neutrophils: Does it matter?* Immunol Rev, 2023. **314**(1): p. 442-456.
15. Carmona-Rivera, C. and M.J. Kaplan, *Induction and Quantification of NETosis.* Curr Protoc Immunol, 2016. **115**: p. 14.41.1-14.41.14.
16. Zuo, Y., et al., *Neutrophil extracellular traps in COVID-19.* JCI Insight, 2020. **5**(11).
17. Mol, S., et al., *Efficient Neutrophil Activation Requires Two Simultaneous Activating Stimuli.* Int J Mol Sci, 2021. **22**(18).
18. Blanter, M., et al., *Method Matters: Effect of Purification Technology on Neutrophil Phenotype and Function.* Front Immunol, 2022. **13**: p. 820058.
19. Hoppenbrouwers, T., et al., *In vitro induction of NETosis: Comprehensive live imaging comparison and systematic review.* PLoS One, 2017. **12**(5): p. e0176472.
20. Damascena, H.L., et al., *Neutrophil Activated by the Famous and Potent PMA (Phorbol Myristate Acetate).* Cells, 2022. **11**(18).
21. Rudd, K.E., et al., *Global, regional, and national sepsis incidence and mortality, 1990-2017: analysis for the Global Burden of Disease Study.* Lancet, 2020. **395**(10219): p. 200-211.

22. Shankar-Hari, M., et al., *Rate and risk factors for rehospitalisation in sepsis survivors: systematic review and meta-analysis.* Intensive Care Med, 2020. **46**(4): p. 619-636.
23. Pryzdial, E.L.G., A. Leatherdale, and E.M. Conway, *Coagulation and complement: Key innate defense participants in a seamless web.* Front Immunol, 2022. **13**: p. 918775.
24. Lv, S., et al., *Anti-TNF-α therapy for patients with sepsis: a systematic meta-analysis.* Int J Clin Pract, 2014. **68**(4): p. 520-8.
25. Hidalgo, A., et al., *Neutrophil extracellular traps: from physiology to pathology.* Cardiovasc Res, 2022. **118**(13): p. 2737-2753.
26. Tsourouktsoglou, T.D., et al., *Histones, DNA, and Citrullination Promote Neutrophil Extracellular Trap Inflammation by Regulating the Localization and Activation of TLR4.* Cell Rep, 2020. **31**(5): p. 107602.
27. Neuenfeldt, F., et al., *Inflammation induces pro-NETotic neutrophils via TNFR2 signaling.* Cell Rep, 2022. **39**(3): p. 110710.
28. Wohlgemuth, L., et al., *Modulation of Neutrophil Activity by Soluble Complement Cleavage Products-An In-Depth Analysis.* Cells, 2022. **11**(20).
29. Ledderose, C., et al., *Optimized flow cytometry assays to monitor neutrophil activation in human and mouse whole blood samples.* J Immunol Methods, 2023. **512**: p. 113403.